NUMERICAL SIMULATIONS OF THICK ALUMINUM WIRE BEHAVIOR UNDER MEGAAMPERE CURRENT DRIVE*

S. F. Garanin[ξ], **S. D. Kuznetsov,**
All-Russian Research Institute of Experimental Physics (VNIIEF), 607190
Sarov, Nizhni Novgorod region, Russia

W. L. Atchison, R. E. Reinovsky,
Los Alamos National Laboratory
Los Alamos, New Mexico, USA

T. J. Awe, B. S. Bauer, S. Fuelling, I. R. Lindemuth, R. E. Siemon
University of Nevada, Reno
Reno, Nevada, USA

Abstract

A series of experiments to study the behavior of thick wires (0.5 mm to 2 mm in diameter) driven by currents of about 1 MA have recently been conducted on the Zebra facility at the University of Nevada, Reno. The objective of these experiments was to study plasma formation on the surface of conductors under the impact of megagauss magnetic fields. Laser shadowgraphy, filtered optical and extreme ultraviolet photodiodes, and extreme ultraviolet spectroscopy used in the experiments provided data on radial expansion of wires and plasma radiation. This paper focuses on numerical simulations of these experiments. Simulations with wires having a diameter of 1.6 mm and less demonstrated plasma formation with temperatures above 3 eV, which is in preliminary agreement with the experiment. For 2 mm diameter wires, although plasma can be observed in the simulations, it has substantially smaller optical thickness than in the simulations of the smaller-diameter wires, and the radiation fluxes prove to be much lower. This can shed light on the experimental results, where the radiation of the 2 mm wires was very weak. The simulated time dependences of the wire radii agree rather well with the experimental results obtained using laser diagnostics and light imaging. The experimental data of the photodiodes also agree well with the simulated time dependence of the detected radiation.

I. INTRODUCTION

The problem of interaction between strong magnetic fields and conductors is of high relevance for many applications, including production of ultrahigh magnetic fields, the use of condensed liners both for fusion research, and for high-energy density applications. The condensed matter liner is the key compression mechanism for MAGO–MTF (Magnetic Compression-Magnetized Target Fusion) [1] systems, and the interaction of the magnetized fusion plasma "target" with the (inside) wall of the liner is of high importance to the potential success of the system. To predict and understand this fusion plasma/wall interaction, it is essential to understand the vacuum magnetic field/wall interaction with the wall produced plasma.

As applied to the high energy density research, the condensed matter liner serves as a driver in cylindrical converging geometry to study the behavior of materials under extreme conditions, such as ultra high magnetic fields, multi-megabar shock waves, and material compression by shells. The precision and predictability of such systems is one of the factors that constrain the applicability of liners, and understanding the field/metal interface behavior is particularly important, because this process is closely related to the seeding and growth of instabilities on the driving surface.

Historically, in many areas, including fusion research, the interaction of intense fields/plasmas with metal or insulator walls has been studied mostly theoretically [2-4], and there have been almost no experiments devoted specifically to the interaction of intense fields/plasmas with walls.

In Ref. [5], the problem of field/metal interface behavior is addressed accounting for both electron thermal conductivity and radiation transport in the metal wall and in the wall-produced plasma at fields of 1-10 MG. The paper shows that proper treatment of the problem requires addressing the processes that draw away the Joule heat from the vacuum-plasma interface (heat conduction and radiation transport); otherwise, the temperature of plasma at the wall-vacuum interface will grow infinitely, and the current will get infinitely skinned in an infinitely thin layer near the surface. Should this be ignored in simulations, the skinning will be limited by non-physical factors, such as the mesh size of the numerical simulation grid, and this may lead to invalid

* Work supported in part by the LANS/VNIIEF Contract #37713-000-02-35, Task Order 037
ξ email: sfgar@vniief.ru

Report Documentation Page

Form Approved
OMB No. 0704-0188

1. REPORT DATE	2. REPORT TYPE	3. DATES COVERED
JUN 2009	**N/A**	**-**

4. TITLE AND SUBTITLE	5a. CONTRACT NUMBER
Numerical Simulations Of Thick Aluminum Wire Behavior Under Megaampere Current Drive	5b. GRANT NUMBER
	5c. PROGRAM ELEMENT NUMBER
6. AUTHOR(S)	5d. PROJECT NUMBER
	5e. TASK NUMBER
	5f. WORK UNIT NUMBER
7. PERFORMING ORGANIZATION NAME(S) AND ADDRESS(ES) **All-Russian Research Institute of Experimental Physics (VNIIEF), 607190 Sarov, Nizhni Novgorod region, Russia**	8. PERFORMING ORGANIZATION REPORT NUMBER
9. SPONSORING/MONITORING AGENCY NAME(S) AND ADDRESS(ES)	10. SPONSOR/MONITOR'S ACRONYM(S)
	11. SPONSOR/MONITOR'S REPORT NUMBER(S)

12. DISTRIBUTION/AVAILABILITY STATEMENT

Approved for public release, distribution unlimited

13. SUPPLEMENTARY NOTES

See also ADM002371. 2013 IEEE Pulsed Power Conference, Digest of Technical Papers 1976-2013, and Abstracts of the 2013 IEEE International Conference on Plasma Science. IEEE International Pulsed Power Conference (19th). Held in San Francisco, CA on 16-21 June 2013., The original document contains color images.

14. ABSTRACT

A series of experiments to study the behavior of thick wires (0.5 mm to 2 mm in diameter) driven by currents of about 1 MA have recently been conducted on the Zebra facility at the University of Nevada, Reno. The objective of these experiments was to study plasma formation on the surface of conductors under the impact of megagauss magnetic fields. Laser shadowgraphy, filtered optical and extreme ultraviolet photodiodes, and extreme ultraviolet spectroscopy used in the experiments provided data on radial expansion of wires and plasma radiation. This paper focuses on numerical simulations of these experiments. Simulations with wires having a diameter of 1.6 mm and less demonstrated plasma formation with temperatures above 3 eV, which is in preliminary agreement with the experiment. For 2 mm diameter wires, although plasma can be observed in the simulations, it has substantially smaller optical thickness than in the simulations of the smaller-diameter wires, and the radiation fluxes prove to be much lower. This can shed light on the experimental results, where the radiation of the 2 mm wires was very weak. The simulated time dependences of the wire radii agree rather well with the experimental results obtained using laser diagnostics and light imaging. The experimental data of the photodiodes also agree well with the simulated time dependence of the detected radiation.

15. SUBJECT TERMS

16. SECURITY CLASSIFICATION OF:			17. LIMITATION OF ABSTRACT	18. NUMBER OF PAGES	19a. NAME OF RESPONSIBLE PERSON
a. REPORT **unclassified**	b. ABSTRACT **unclassified**	c. THIS PAGE **unclassified**	**SAR**	**6**	

Standard Form 298 (Rev. 8-98)
Prescribed by ANSI Std Z39-18

and paradoxical results. The paper also shows that at the magnetic fields above approximately 3 MG, plasma of electron-volt temperature forms in a thin layer at the field/metal interface, and the temperature increases with field growth. Experimental data would be very helpful for validating the conclusions of Ref. [5].

Over the last two years, the University of Nevada, Reno (UNR) has conducted a series of experiments [6] with megagauss magnetic fields on the Zebra pulsed power facility. In these experiments, "thick" wires with diameters ranging from 0.5 to 2.0 mm, i.e. wires with the radius bigger than the skin layer, were driven by a current of about 1 MA with a rise time about 100 ns. The field in the conductor reached 4 MG and the magnetic pressure exceeded 0.5 Mbar. The experiments involved a wide range of diagnostics, including current probes, streaked imaging of optical emission, 4-frame laser shadowgraphy, fast photomultipliers, 2-frame optical imaging, green filtered photodiodes, filtered extreme ultraviolet photodiodes, and extreme ultraviolet spectroscopy.

We have performed 1D numerical simulations of these experiments. Simulated data on the emission in the visible and extreme UV ranges, radial wire expansion, and plasma formation are compared here with the experimental data.

II. PROCESSES ADDRESSED AND APPROXIMATIONS

The numerical simulations were performed in cylindrical 1D geometry with an azimuthal magnetic field. The simulations included the MHD motion, the magnetic diffusion, the electron heat conductivity (including this accounting magnetizing), and the radiation transport in the "back-and-forth" approximation. The state of matter was described in the one-temperature approximation, the material strength was ignored.

The equation of state (EoS) used in the simulations is given in Ref. [7]. It has an analytic form. The pressure p and the specific internal energy ε in this equation are sums of three terms, which depend on temperature T and density ρ: a cold, or elastic, term (it represents the condensed density, sonic speed, and the sublimation energy); a hot term coinciding with the Saha EoS for multiply ionized plasma [8] (which defines the EoS for high temperatures or low densities); and a lattice term expressed as $\varepsilon_3 \sim p_3/\rho \sim T^\alpha/\rho^\beta$, where $\alpha < 1$, $\beta < 0$ (this term contributes to the specific heat of the condensed matter and decreases relatively at high temperatures or low densities in the plasma area). The first and the third term of the EoS exactly satisfy the thermodynamic identity, so the error in satisfying the identity is determined only by the Saha equation and should be small. When this EoS is used, the code ordinary does not use two-phase states and, consequently, the Maxwell rule, and it is assumed that the matter in unstable states $\partial p/\partial \rho < 0$ in different grid cells will decompose by itself to gas and condensed phases. The advantage of this approach is that the matter in the two-phase region in simulations will be non-uniform, as it happens in reality. The drawback is that in meta-stable states, if the condition $\partial p/\partial \rho < 0$ is not satisfied, there will be no decomposition to phases, i.e. the lifetime of these meta-stable conditions is assumed to be infinite, which cannot be always assumed true for experimental conditions.

The material resistance used in simulations is determined in different ways for the plasma and condensed state. The resistance of the plasma state is considered to be of Spitzer type with the non-ideality correction and accounting for electron scattering on neutral atoms. For the condensed state, resistance is considered proportional to the internal energy and inversely proportional to the density. For intermediate states, interpolation is made between the formulas for the condensed and the plasma states.

The electron thermal conductivity was determined in the simulations via the electrical conductivity using the Wiedemann-Franz law. In addition, a number of simulations included effects of plasma magnetizing on the electron thermal conductivity using the formulas that approximate the dependence [9] of electron thermal conductivity on the degree of plasma magnetizing.

Radiation transport in the simulations was determined in the "back-and-forth" approximation [8]. In the simulations, we used the radiation path of a continuous spectrum for the multiple ionization [8] averaged according to Rosseland, which had the form:

$$l = a\frac{T^{7/2}A^2}{\rho^2(z+0.0001)^2 z^*}, \text{ where } z^* = \begin{cases} z, & z > 1 \\ 1, & z \le 1 \end{cases}, \qquad (1)$$

where z is ion charge, A is atomic weight. In a number of simulations, in order to include to some extent the influence of lines on plasma cooling and radiation transport, the coefficient in formula (1) was reduced compared to [8].

The accuracy of the equation of state and transport coefficient formulas used in the simulations is not very high, but the goal of our work was to use wide-range dependencies with proper asymptotic forms to produce qualitatively correct results. Of importance was to incorporate all essential physical processes for qualitative description of the 1D problem.

III. PROBLEM STATEMENT

1D numerical simulations were used to study the behavior of cylindrical aluminum wires of different diameter: 0.5; 1; 1.6; 2 mm driven by currents of the Zebra generator. The generator current waveform [10] in the experiments was almost independent of the load; therefore, the simulations were performed with a typical

waveform shown in Fig. 1.

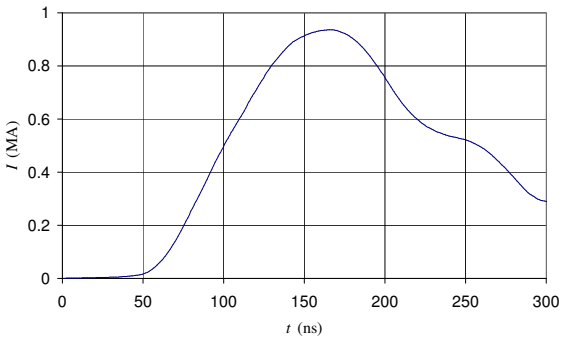

Figure 1. Zebra current waveform used in the simulations.

The simulations were performed using the 1D Lagrangian MHD code UP-MHD [5].

At the plasma/vacuum interface, the density of matter tends to zero. Therefore, to describe this region in the Lagrangian simulations, it was necessary to have very fine grid at the beginning (in the condensed state). In the simulations we used varied-mass mesh size with a growing density of meshes towards the plasma/vacuum interface. When transforming to plasma, the meshes at the interface expanded, and their spatial size became not very small. Another argument in favor of using rather a fine grid is related to the fact that in order to describe the thermal breakdown (if it occurs inside the two-phase region) in the simulations, gas and liquid meshes in the two-phase region should have enough time to equalize their temperatures via the electron thermal conductivity to avoid cooling of gas meshes as a result of their expansion and to enable plasma formation in them due to the Joule heating. As a result for the wires with a diameter 1 mm and smaller, we managed to obtain rather good convergence with a number of meshes of about 1200 with mass decrement towards the vacuum 0.9933 (in this case for the 1 mm diameter wire the minimum mesh size at the plasma/vacuum interface was 0.001 μm). An example of density, magnetic field and temperature profiles for the 1 mm diameter wire simulations accounting for electron thermal conductivity magnetizing, which was obtained in the simulations with a different number of meshes (400, 600 and 1200, with the same largest/smallest mesh size ratio in all the simulations) at time $t = 200$ ns is shown in Fig. 2. This figure shows rather good convergence of the results. Note that the initial breakdown observed in the experiment probably occurred at the expanding wire vapor/vacuum interface, rather than in the two-phase region, in accordance with arguments presented in Ref. [5]. The breakdown in this case was described phenomenologically, and this description probably does not require such a fine grid.

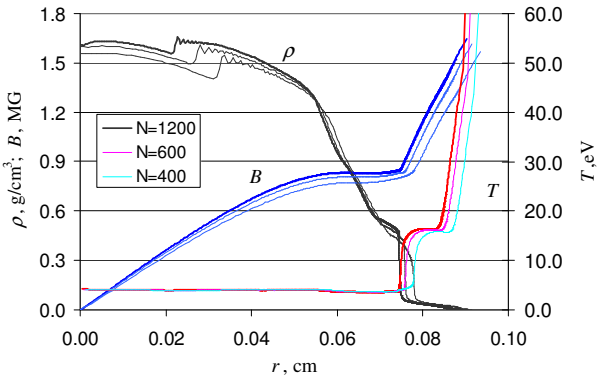

Figure 2. Density, magnetic field, and temperature profiles for the 1 mm wire obtained in the simulations with a different number of meshes (400, 600 and 1200) at time $t = 200$ ns.

IV. SIMULATIONS OF WIRES AND PLASMA FORMATION

We have performed a number of simulations for the experiments on Zebra, in which we varied some parameters. We have showed that thermal conductivity magnetizing has almost no effect on the simulation results. Therefore, we will present simulation results that do not account for thermal conductivity magnetizing. Although the radiation path also had a minor effect on the simulation results, we will nevertheless present the simulation results with the path reduced by a factor of 4 compared to [8] in order to incorporate the contribution of the line spectrum into cooling of optically thin plasma and its influence on the Rosseland path for optically thick plasma. It became clear during the simulations that as the vaporization temperature in our EoS model is noticeably overestimated, plasma in the simulations was observed to form in the two-phase liquid-gas region, which does not completely agree with experimental data, such as time dependence of the wire diameter and emission from wires in visible and extreme UV range at the initial stage of plasma formation. Apparently, a considerable quantity of relatively cold vapor formed at the initial stage of the experiments. In order to reduce the vaporization temperature, we changed the speed of sound c_0 used in our EoS to $c_0 = 0.4$ cm/μs (instead of $c_0 = 0.5$ cm/μs). To enable the breakdown of the cold non-conducting vapor at the plasma/vacuum interface in accordance with arguments of Ref. [5] in the simulations, we introduced a bottom limit for conductivity, $\sigma_{\min}$. This quantity should be treated as a phenomenological parameter, because description of a real breakdown requires that there should be at least a detailed description of radiation transport from the two-phase (or hot condensed) region through cold vapor to the plasma/vacuum interface as a mechanism, by which ionization is seeded at the

plasma/vacuum interface. Selection of this quantity for the description of the experimental breakdown will depend on the spatial grid used in the simulation, because for any finite conductivity Joule heating per gram of matter for an infinitely fine grid will be infinite, and the breakdown will consequently be instantaneous.

The simulations with $c_0 = 0.4$ cm/μs and $\sigma_{min} = 0$ show that plasma forms only for wires with diameters less than 1 mm. By fitting respective values of σ_{min} in the simulations, we described the experimental time of breakdown for 0.5, 1 and 1.6 mm diameter wires. Experimental data seems to show that there was no plasma formation for the thickest 2 mm diameter wire, so σ_{min} was chosen so that there was no breakdown for these experiments. Fig. 3 shows simulation results for the 1 mm diameter wire for the breakdown at the plasma/vacuum interface.

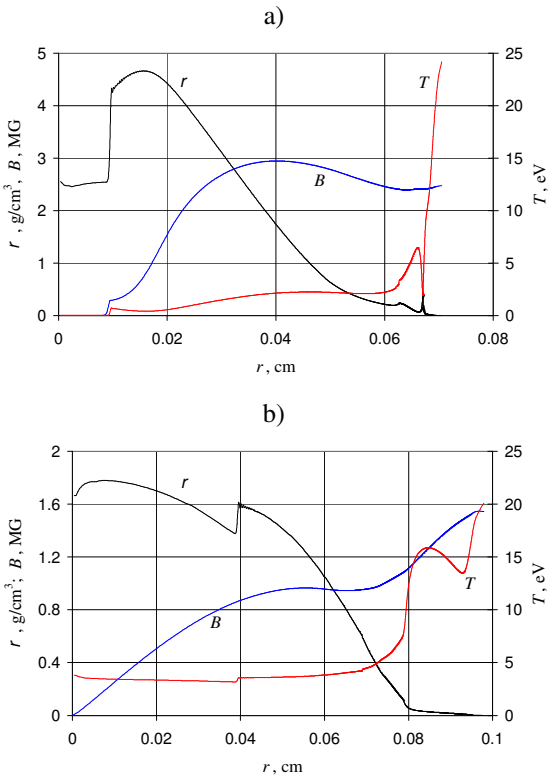

Figure 3. Density, magnetic field, and temperature profiles for the 1 mm diameter wire at times: a) $t = 140$ ns ; b) $t = 200$ ns .

The spread of plasma region towards the wire center for small-diameter wires (0. 5 mm и 1 mm) rather quickly takes the form of a thermal conductivity wave (Fig. 3b) having an optical thickness of many photon paths, so the use of Rosseland paths in this case seems appropriate. For the 1.6 mm diameter wire, the solution with radiant thermal conductivity was approached only at the end of the simulation run, when the current was much smaller; and for the 2 mm diameter wire, the optical thickness of the plasma region even by $t = 300$ ns was still small.

Because of the substantial difference in the role of the plasma region and strongly different temperatures for wires with different diameters, radiation fluxes from the wires prove to be strongly different. This is illustrated in Fig. 4, which shows radiation fluxes as a function of time per unit wire length for different-diameter wires. For 2 mm diameter wire the radiation emission was very weak (less than 10^{-5} J/cm/ns) and probably it was hard to detect it in the experiment.

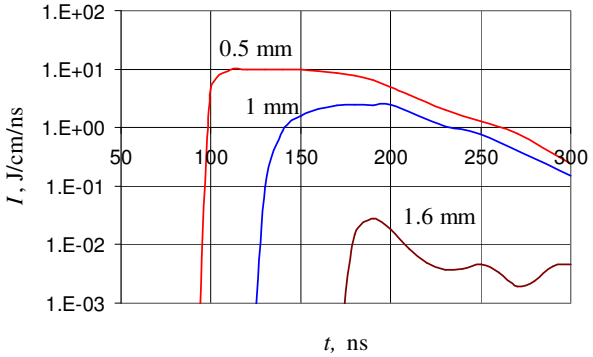

Figure 4. Radiation fluxes per unit wire length as a function of time.

V. COMPARISON OF SIMULATED AND EXPERIMENTAL DATA

Simulation results allow comparing a number of parameters with experimental data. Fig. 5 shows the simulation time dependences of the wires' external radii and the experimental points. Simulated values agree with the experimental ones.

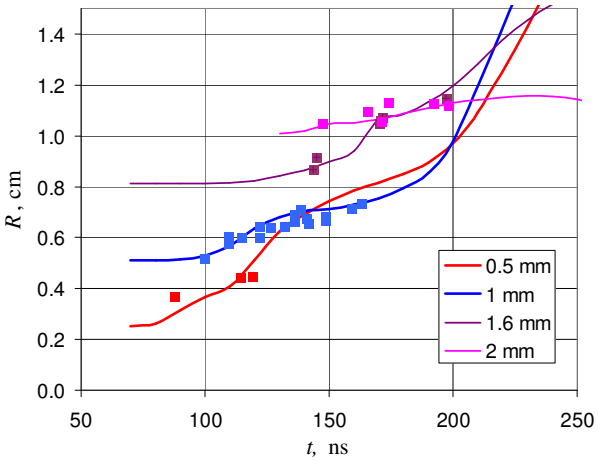

Figure 5. Time dependences of the simulated and experimental wires' radii.

The simulation data were also used to determine the green-filtered photodiode currents. The problem is

reduced to integrating the radiation spectrum over a filter transmission band and over the wire cross-section accounting for the radiation absorption in the outer layers.

Let us find the spectrum of radiation emitted by the wire in the frames of the used back-and-forth and gray matter approximation. The total intensity of radiation emitted by the layer of matter with the thickness dr is

$$2\sigma_{SB}T^4 d\xi = 3\sigma_{SB}T^4 \frac{dr}{l}, \qquad (2)$$

where σ_{SB} is the Stefan-Boltzmann constant, $\xi = 1.5\int \frac{dr}{l}$ is optical thickness, which has a factor of 1.5 in the back-and-forth approximation to provide correct limiting transition to the diffusion equation. Since in the gray matter approximation (when the absorption coefficient depends only on temperature and density) the emission spectrum should coincide with the black-body spectrum. The spectrum of radiation emitted by a layer of the matter with the thickness dr can be obtained by distributing the intensity (2) over the black-body radiation spectrum, i.e. by multiplying (2) by dE_ω^{BB}/E^{BB}, where dE_ω^{BB} and E^{BB} are the energy of black-body radiation in the spectral interval $d\omega$ and the total energy of black-body radiation. By substituting these quantities [8], we obtain the spectral composition of radiation emitted by the layer dr, and then the spectrum of radiation incident on the sensor integrating this spectral intensity over the volume with account for the radiation absorption in the wire material. Since radiation observed in the experimented was emitted by a small area of the surface and perpendicular to the surface, the radiation spectrum in the frames of the considered model can be determined by the integral

$$dI_\omega \sim \omega^3 d\omega \int \frac{dr}{l} \frac{1}{(\exp(\hbar\omega/kT)-1)} \exp\left(-\int_r^\infty \frac{dr'}{l}\right), \qquad (3)$$

where $\int_r^\infty \frac{dr'}{l}$ is the optical thickness counted down from the wire surface, without the factor of 1.5, which was used in the back-and-forth approximation.

In order to obtain time dependences of green-filtered diode currents and compare these currents in different experiments, in the formula (3) one should use a frequency interval in the region of $\hbar\omega = 2.34$ eV corresponding to the wavelength 530 nm, and the values of these currents I_d will then be determined as

$$I_d \sim \int \frac{dr}{l} \frac{1}{(\exp(\hbar\omega/kT)-1)} \exp\left(-\int_r^\infty \frac{dr'}{l}\right). \qquad (4)$$

A calibration of the diodes showed that for high diode currents there is essential nonlinear correction. Fig. 6 presents experimentally found relation between the linear current (4) and the diode current measured in experiments.

Fig. 7 shows simulated green-filtered diode currents incorporating this nonlinear correction compared with the experimental curves. The simulated currents for small diameter wires (0.5 and 1 mm) are in good agreement with the experimental ones.

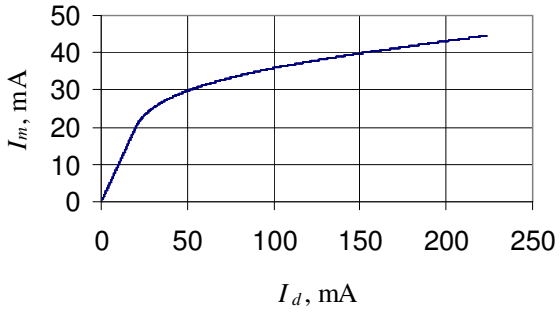

Figure 6. Relation between of the linear current and the diode current I_m measured in the experiment.

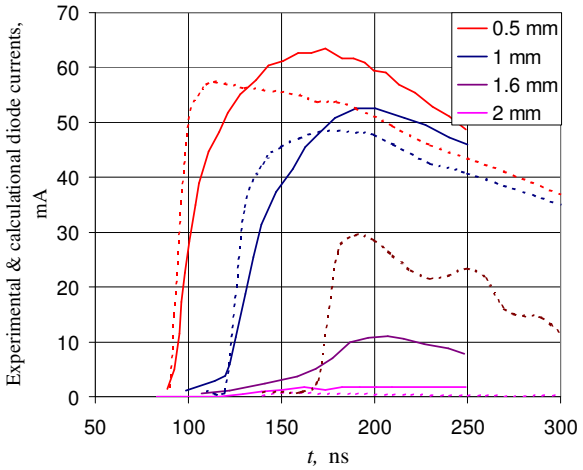

Figure 7. Experimental (solid curves) and simulated (dashed curves) green-filtered diode currents vs. time. Simulated diode currents are normalized by the condition: the linear diode current I_d equal to 30 mA corresponds to the black-body wire temperature of 2.4 eV .

The curves shown in Fig. 7 take into account the correction related to geometric effects, which come into play, when the image of the thin wire does not cover the entire width of the diode surface. We included these effects in the simulations in a qualitative way, assuming the signal to be proportional to the wire surface, which is seen by the diode. In this case, the magnification of the wire image by a factor of 5.6 at its projecting through a lens to a diode area of 4.4 mm should reduce the current $R/0.39$ mm times, if the radius of the wire's emitting region R is smaller than 0.39 mm. This effect manifested itself only in the signal from the 0.5 mm diameter wire. The simulated curves shown in Fig. 7 were normalized in such a way that the 2.4 eV black-body emission from the wires in experimental geometry corresponded to the linear diode current I_d of 30 mA.

The experiments also provided data on EUV emission from the wires. These data were obtained by AXUV photodiodes with aluminum (200 nm) and silicon/zirconium (100 nm/200 nm) filters, whose spectral response is shown in Fig. 8.

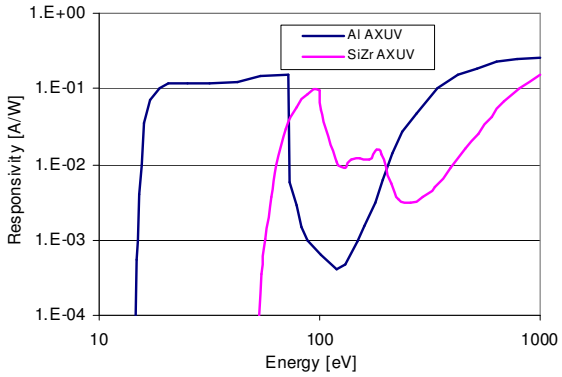

Figure 8. Filtered AXUV photodiode spectral response.

A comparison of simulated and experimental photodiode signals behind these filters for the 1 mm wire experiment is presented in Fig. 9, where the simulated curves are normalized so that the aluminum-filtered peak signal approximately coincides with the experimental one. In this case, one should compare the waveform and the relative amplitude of aluminum and silicon/zirconium filtered diode signals. When comparing the results, one should note that the difference between experimental pulse widths in different experiments was about 30 %. Given this, the results also demonstrate good agreement.

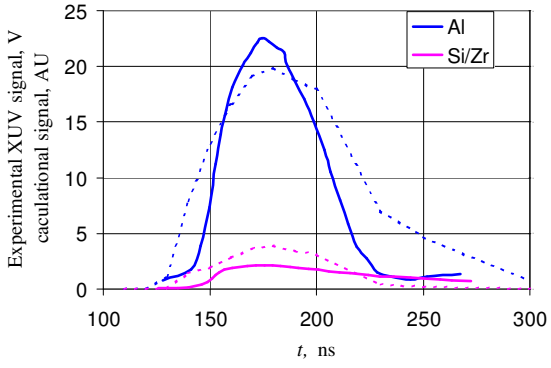

Figure 9. EUV plasma emission from 1-mm wire. Filtered diode signals in the experiment (solid lines) and simulation (dashed lines).

VI. CONCLUSIONS

In order to provide convergence of simulations and correct description of the wire behavior, including the onset of plasma formation (if thermal breakdown of the wire occurs inside the two-phase region), one should use very high-resolution spatial grids. Simulations of the thick-wire behavior incorporating plasma formation in the Zebra experiments with mega-ampere current show good agreement with the experiments.

Based on this agreement, one can draw a conclusion that in agreement with the simulation results plasma on the wire surface formed for all the wire diameters studied in the experiments, except probably the 2 mm diameter wire, where the magnetic field did not exceed 2 MG . However, it is probably rather difficult to detect plasma formation in wires with such diameters, because – as suggested by the simulations – radiation fluxes for them prove to be several orders smaller than for the wires with a smaller diameter even if plasma formation take place.

VII. REFERENCES

[1] S. F. Garanin, V. I. Mamyshev, and V. B. Yakubov, "The MAGO system: current status," IEEE Trans. Plasma Sci. vol. 34, pp. 2273-2278, 2006.

[2] S. F. Garanin, "Diffusion of a strong magnetic field in a dense plasma," J. Appl. Mech. Tech. Phys., No. 3, pp. 308-312, 1985.

[3] G. E. Vekshtein, "Magnetic and thermal processes in dense plasma" (in Russian), in Rev. Plasma Phys., vol. 15, B. B. Kadomtsev, Ed., Moscow: Energoatomizdat, 1987, pp. 3-54.

[4] S. F. Garanin and V. I. Mamyshev, "Cooling of a magnetized plasma at a boundary with an exploding metal wall," J. Appl. Mech. Tech. Phys., No. 1, pp. 28-34, 1990.

[5] S. F. Garanin, G. G. Ivanova, D. V. Karmishin, and V. N. Sofronov, "Diffusion of a megagauss field into a metal," J. Appl. Mech. Tech. Phys., vol. 46, pp. 153-159, 2005.

[6] T. J. Awe, B. S. Bauer, R. E. Siemon, et al., "Plasma formation and evolution from thick aluminum wires pulsed with megagauss field," presented at XII Int. Conf. on Megagauss Magnetic Field Generation and Related Topics, Novosibirsk, Russia, 2008.

[7] A. M. Buyko, S. F. Garanin, V. A. Demidov, et al., "Investigation of the dynamics of a cylindrical exploding liner accelerated by a magnetic field in the megagauss range," in Megagauss Fields and Pulsed Power Systems, V. M. Titov and G. A. Shvetsov, Ed., New York: Nova Science Publishers, 1990, p. 743.

[8] Ya. B. Zel'dovich and Yu. P. Raizer, Physics of shock waves and high-temperature hydrodynamic phenomena. Vol. 1. New York: Academic Press, 1966.

[9] S. I. Braginsky, "Transport processes in a plasma," in Rev. Plasma Phys., vol. 1, New York: Consultants Bureau, 1965, p. 205.

[10] S. Fuelling, T. J. Awe, B. S. Bauer, et al., "A Zebra experiment to study plasma formation by megagauss fields," IEEE Trans. Plasma Sci. vol. 36, pp. 62-69, 2008.